

1 **Projected increases in wildfires may challenge regulatory curtailment of PM_{2.5} over the**
2 **eastern US by 2050**

3

4 Chandan Sarangi^{1,2,3*}, Yun Qian^{3*}, L. Ruby Leung³, Yang Zhang⁴, Yufei Zou^{5,3}, Yuhang
5 Wang⁵

6

7 ¹ Indian Institute of Technology (IIT) Madras, Chennai, India

8 ²Laboratory of Atmospheric and Climate Sciences, IIT Madras, Chennai, India

9 ³ Pacific Northwest National Laboratory, Richland, WA, USA

10 ⁴ Department of Civil and Environmental Engineering, Northeastern University, Boston, MA

11 ⁵ School of Earth and Atmospheric Sciences, Georgia Institute of Technology, Atlanta, GA,
12 USA.

13

14

15 *Corresponding Authors:

16 chandansarangi@iitm.ac.in

17 yun.qian@pnnl.gov

18

19

20

21

22 **Abstract**

23 Anthropogenic contribution to the overall fine particulate matter (PM_{2.5}) concentrations has
24 been declining sharply in North America. In contrast, a steep rise in wildfire-induced air
25 pollution events with recent warming is evident in the region. Here, based on coupled fire-
26 climate-ecosystem model simulations, summertime wildfire-induced PM_{2.5} concentrations are
27 projected to nearly double in North America by the mid-21st century compared to the
28 present. More strikingly, the projected enhancement in fire-induced PM_{2.5} (~ 1-2 µg/m³) and
29 its contribution (~15-20%) to the total PM_{2.5} are distinctively significant in the eastern US.
30 This can be attributed to downwind transport of smoke from future enhancement of wildfires
31 in North America to the eastern US and associated positive climatic feedback on PM_{2.5} i.e.
32 perturbations in circulation, atmospheric stability and precipitation. Therefore, the anticipated
33 reductions in PM_{2.5} from regulatory controls on anthropogenic emissions could be
34 significantly compromised in the future in the densely populated eastern US.

35 **Key points:**

- 36 1) Wildfire-PM_{2.5} associations studied based on unprecedented two-way coupled fire-
37 climate-ecosystem model simulations
- 38 2) A steep rise in wildfire-induced air pollution events with recent warming is evident in
39 the region
- 40 3) The transported smoke from enhanced wildfires in North America can severely affect
41 air quality over Eastern US

42

43 **Keywords:** wildfire emissions, climate change, air quality, smoke transport, wildfire-climate-
44 ecosystem interactions

45 **1. Introduction**

46 Wildfires are widespread burning events in forests, shrub lands, and grazing lands. In
47 North America (mainly Canada and the US), particulate matter emissions from wildfires are a
48 significant source of regional air pollution (Shi et al., 2019; McClure and Jaffe, 2018; Van
49 Der Werf et al., 2010; Jaffe et al., 2008). Since the 1980s, the number of large wildfires and
50 the length of wildfire season have been increasing, and the trends are projected to continue in
51 the future over the western US, Alaska and Canada (Kitzberger et al., 2017; Kirchmeier-
52 Young et al., 2017; Abatzoglou and Williams, 2016; Partain et al., 2016; Jolly et al., 2015;
53 Westerling et al., 2006; Gillett et al., 2004). Accordingly, particulate emissions from wildfires
54 are also anticipated to increase in North America in the 21st century (Knorr et al., 2017; Liu
55 et al., 2016; Val Martin et al., 2015). Human exposure to high concentrations of wildfire-
56 emitted airborne particulate matter of diameter $\leq 2.5 \mu\text{m}$ (PM_{2.5}) is known to have substantial
57 adverse effects on pulmonary and cardiovascular functioning (Anjali et al., 2019; Black et al.,
58 2017), which contribute significantly to global and regional all-cause mortality (Zhang et al.,
59 2020; Hong et al., 2019; Yang et al., 2019; Ford et al., 2018; Johnston. et al., 2012).
60 Therefore, a better understanding of the future changes in wildfire-induced PM_{2.5} and its
61 contribution to the total surface PM_{2.5} is essential.

62 In the last two decades, ambient air quality in the US has substantially improved due
63 to a decline in PM_{2.5} by ~ 40 % (US EPA, 2018). The decrease in PM_{2.5} is primarily due to
64 curtailment of anthropogenic emissions resulting from US-based efforts to meet regulations
65 such as the Clean Air Act (US EPA, 2009), Cross-State Air Pollution Rule, Regional Haze
66 Rule, and the motor vehicles emissions standards. Consequently, air quality over the

67 contiguous US (CONUS) and Canada has improved steadily such that it is predicted to
68 achieve the targeted National Ambient Air Quality Standards in the future (Nolte et al.,
69 2018). Under this promising scenario, the influence of wildfire-emissions on the total $PM_{2.5}$
70 becomes even more crucial. Depending on the competition between climate-induced increase
71 in wildfires and the regulatory control on anthropogenic emissions, future enhancement in
72 wildfire-induced $PM_{2.5}$ may compromise the reduction in anthropogenic $PM_{2.5}$ concentrations
73 in certain regions. In agreement, recent studies have highlighted the potential for future
74 enhancement in wildfire-induced pollution to diminish the reducing trend in $PM_{2.5}$, primarily
75 over the western US (O'Dell et al., 2019; Ford et al., 2018; Val Martin et al., 2015; Yue et al.,
76 2013).

77 While the fractional wildfire burnt area and fire intensities are the greatest over the
78 western US and Canadian regions within North America, anthropogenic emissions dominate
79 the ambient $PM_{2.5}$ concentration over the eastern US. The inherent geographical separation
80 between the regions with large wildfire emissions and anthropogenic emissions leads to a
81 pertinent question: will future enhancement in wildfires over the western US and Canada
82 have significant effects on $PM_{2.5}$ over the eastern US? Addressing this question is crucial
83 because the declining trend in $PM_{2.5}$ over the eastern US is the major contributor to the
84 observed 40% decrease in $PM_{2.5}$ over the US in the last two decades (US EPA, 2018).
85 Eastward advection of wildfire smoke from Canada and the western US has been found to
86 severely hamper the surface air quality of the central and eastern US under the influence of
87 the prevailing westerlies during the summer months (Brey et al., 2018; Wu et al., 2018;
88 Gunsch et al., 2018; Kaulfus et al., 2017; Dempsey, 2013). The transported wildfire smoke
89 can influence the meteorology and climate via the radiative impact of carbonaceous
90 emissions, changes in land albedo and cloud system perturbations (Ward et al., 2012; Liu et
91 al., 2014). These fire-weather interactions can have positive feedback on the locally-emitted

92 PM_{2.5} in the eastern US by surface cooling and boundary layer suppression(Guan et al.,
93 2020). At the same time, fire-triggered ecosystem changes can induce negative feedback on
94 PM_{2.5} by reducing the future wildfires over North America (Zou et al., 2020). Thus, two-
95 way interactions between fires and climate that are important for predicting future changes in
96 wildfire locations, intensities, and durations (Harris et al., 2016) as well as associated
97 particulate emissions is essential. However, past studies have mostly employed simple
98 statistical models based on statistical regressions of present-day fire burnt area on the
99 meteorological fields (Liu et al., 2016; Spracklen et al., 2009; Yue et al., 2013; Val Martin et
100 al., 2015), and more recently, one-way coupled modelling (Ford et al., 2018; O’Dell et al.,
101 2019).

102 Here, based on new two-way coupled fire-climate-ecosystem simulations, we
103 demonstrate the significance of wildfire-induced contributions to ambient PM_{2.5} over the
104 eastern US due to enhanced wildfire smoke transportation and smoke-induced changes in
105 weather in eastern US. This enhancement in wildfire-induced PM_{2.5} may potentially challenge
106 the targeted policy-driven reduction of PM_{2.5} in the eastern US. Next, our model setup,
107 experiments and methodology are explained in Section 2, followed by results and discussion
108 in Section 3. The study is summarized in Section 4.

109 **2. Materials and Methods**

110 **2.1. RESFire-CESM Model description**

111 We employ the open-source REgion-Specific ecosystem feedback fire (RESFire)
112 model coupled with the Community Land Model version 4.5 and the Community
113 Atmosphere Model version 5 (CAM5) of the Community Earth System Model (CESM)
114 version 1 (Zou et al., 2019; Neale et al., 2013) to perform two-way coupled simulations.
115 RESFire provides state-of-the-art capabilities to simulate the complex fire-climate-ecosystem

116 interactions globally for fires occurring over wildland, cropland, and peatland. Although
117 wildfires dominate in the North American region, RESFire simulates both wildfires and
118 prescribed fires. Moreover, this integrated setup includes climatic feedback from fire-induced
119 aerosol direct and indirect radiative effects and associated weather changes. It also includes
120 feedback from fire-induced vegetation distribution changes and associated biophysical
121 processes such as evapotranspiration and surface albedo. Sofiev et al. (2012) described the
122 fire plume rise parameterization. Other features in CLM4.5 and CAM5, such as the
123 photosynthesis scheme (Sun et al., 2012), the MAM3 aerosol module (Liu et al., 2012), and
124 the cloud macrophysics scheme (Park et al., 2014), allow for more comprehensive
125 assessments of the climate effects of fires through their interactions with vegetation and
126 clouds. Fire-ecosystem interactions are modelled by simulating fire-induced vegetation
127 mortality and regrowth (and associated land cover change) in RESFire. This approach has
128 been introduced in Zou et al. (2019) and the simulated ecological and climatic effects of
129 wildfires have been evaluated in two sets of sensitivity experiments in Zou et al. (2020).
130 Although fire-climate-ecosystem interactions are considered in this study, our focus is on the
131 fire-induced changes in PM_{2.5} over Canada and the US, so the two vegetation-focused
132 sensitivity experiments reported in Zou et al. (2020) are not included in this paper. Please
133 refer to Zou et al. (2019) and Zou et al. (2020) for more details about the simulation of fire-
134 ecosystem interactions.

135 **2.2 Numerical Experiment and Methodology**

136 We designed two sets of simulations for the present day and future scenarios to
137 quantify the impacts of fire-climate-ecosystem interactions (Table 1). The spatial resolution is
138 0.9° (lat) \times 1.25° (lon) with a time step of 30 min. In each set of simulations, we conducted a
139 default all emission included control run (X_{ALL}, where x=2000 or 2050 indicates the present
140 day or future, respectively) and a sensitivity run with no wildfire emissions to the atmosphere

141 (X_{WEF} , where X is the same as for the control runs). The ALL runs are designed to simulate
 142 fully interactive fire disturbances such as fire emissions with plume rise and fire induced land
 143 cover changes of the present day (representative of the 2000s, 2000_{ALL}) and a moderate future
 144 emission scenario (representative of the 2050s, 2050_{ALL}) via the RCP4.5. The only difference
 145 between the ALL and WEF scenario is that wildfire emissions are absent in the WEF
 146 scenario. Specifically, in the WEF runs, the online simulated fire emissions are not passed to
 147 the CAM5 atmosphere model so that the difference between the ALL and WEF runs can be
 148 used to isolate the atmospheric impacts of fire-climate interactions.

149 Table 1: Summary of the sensitivity simulations performed

Scenario	Present-day		Future	
Experiment Name	2000_{ALL}	2000_{WEF}	2050_{ALL}	2050_{WEF}
Simulation years	2001-2010	2001-2010	2051-2060	2051-2060
Atmosphere	CAM5	CAM5	CAM5	CAM5
Land	CLM4.5	CLM4.5	CLM4.5	CLM4.5
Ocean	Climatology	Climatology	RCP4.5	RCP4.5
Sea ice	Climatology	Climatology	RCP4.5	RCP4.5
Non-fire emissions	ACCMIP	ACCMIP	RCP4.5	RCP4.5
Fire emissions	Online fire aerosols with plume rise	—	Online fire aerosols with plume rise	—
Land cover	Fire disturbances on present-day condition	Fire disturbances on present-day condition	Fire disturbances on RCP4.5 condition	Fire disturbances on RCP4.5 condition

150

151 For the present-day experiments, we used the spun-up states from Zou et al. (2019) as
 152 initial conditions for both meteorological and chemical variables. Sea surface temperature
 153 (SST) for the present day was obtained from the Met Office Hadley Centre (HadISST).
 154 Present-day non-fire emissions from anthropogenic and other sources were based on
 155 ACCMIP (Lamarque et al., 2010) for the year 2000. We replaced the prescribed GFED2 fire
 156 emissions (van der Werf et al., 2006) in the default setting of CESM with the online-coupled

157 fire emissions generated by the RESFire model. Zou et al. (2019) provided more details of
158 the physics parameterizations and modeling experiment settings used in these simulations.
159 Land use and land cover data for 2000 and 2050 from the Land-Use History A product (Hurtt
160 et al., 2006) are used to initialize the 2000_{ALL}/2000_{WEF} and 2050_{ALL}/2050_{WEF} simulations,
161 respectively. Following the above setup, the future scenario 2050_{ALL} experiment accounts for
162 both fuel load changes associated with the projected land use and land cover change
163 (LULCC) in the 2050s and fire weather changes driven by the SST and sea ice forcing from a
164 coupled CESM simulation following the greenhouse gas (GHG) forcing of the RCP4.5
165 scenario. The global mean GHG mixing ratios in the CAM5 atmosphere model were fixed at
166 the year 2000 levels in all the present-day experiments and they were replaced by those of the
167 RCP4.5 scenario with the well-mixed assumption and monthly variations. However, the
168 future population and socioeconomic conditions were identical to those of the present day so
169 there was no explicit impact of human-induced mitigation/enhancement effects on wildfires
170 in the future projection in all the future experiments. Future human impacts were considered
171 implicitly in LULCC-induced fuel load changes in the RCP4.5 scenario.

172 The net projected changes by 2050s in emissions, meteorology and air quality during
173 summer (JJA: June, July, August) months are estimated by comparing decadal-mean values
174 simulated by 2000_{ALL} with 2050_{ALL}. Wildfire-induced enhancement in PM_{2.5} concentration in
175 the present day and mid-21st century is estimated by comparing 2000_{ALL} with 2000_{WEF} and
176 2050_{ALL} with 2050_{WEF}, respectively. Further, the projected increase in wildfire-induced
177 PM_{2.5} in the future is calculated by comparing the simulated wildfire effect of the 2050s
178 (2050_{ALL}-2050_{WEF}) with that of the 2000s (2000_{ALL}-2000_{WEF}). With large spatiotemporal
179 variability, the projected changes in transported fire-emissions from the western US and
180 Canada to the eastern US by the 2050s and the corresponding impacts are summarized using

181 probability distribution functions. The latter provide information not only for the mean but
182 also variability and extreme values to quantify the simulated changes for the three subregions.

183

184 **3. Results and Discussion**

185 **3.1 Model Evaluation**

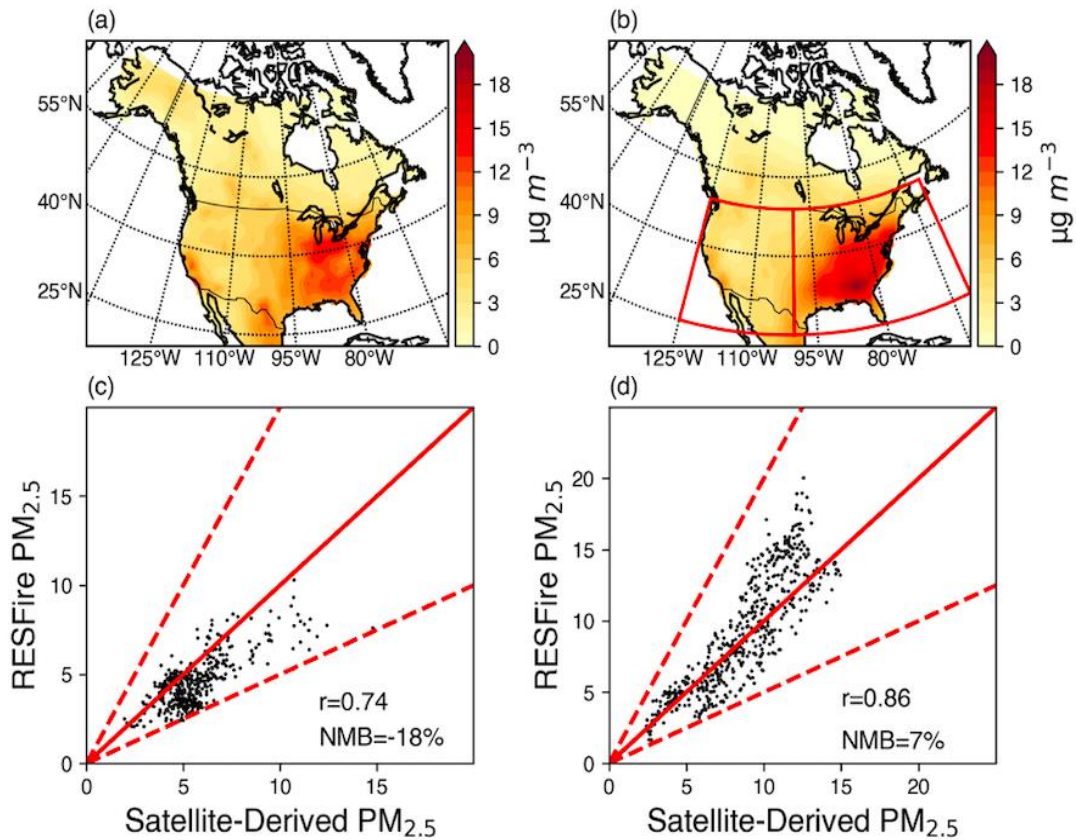
186 Zou et al. (2019) performed comprehensive evaluation of the RESFire simulated
187 wildfire burnt area distribution, associated carbon emissions and terrestrial carbon balance to
188 demonstrate reasonable model skill. Zou et al. (2020) compares global fire simulations by
189 CESM-RESFire with modeling results reported in the literature to show better agreement
190 with the GFED4.1s benchmark data and predicts more prominent changes in the future than
191 those predicted by Kloster et al. (2010, 2012). These differences might come from differences
192 in the climate sensitivities of the fire models and scenarios and other input data used to make
193 future projections.

194 Here, we evaluate the simulated surface $PM_{2.5}$ against satellite-estimates (Figure 1)
195 over North America. The $PM_{2.5}$ concentration is calculated as the sum of sulfate, nitrate, fine
196 sea salt (first 2 size bins), fine dust (first size bin), black carbon (BC), and organic aerosol
197 (OC) at the surface-level of model. OC is the sum of primary organic matter (POM) and
198 secondary organic aerosol (SOA), and SOA is the sum of secondary species formed from
199 toluene, monoterpenes, isoprene, benzene, and xylene. Figure 1 compares the observed and
200 simulated mean annual $PM_{2.5}$ averaged over 2001-2010. The 10-year average satellite AOD-
201 derived annual mean surface $PM_{2.5}$ concentrations (Van Donkelaar et al., 2018) are regridded
202 to the model grid (Figure 1A) and then compared with the RESFire simulations in the
203 2000_{ALL} present-day run (Figure 1B). The spatial distribution of annual surface $PM_{2.5}$ is
204 reasonably well simulated but also have some biases. To quantify the biases, we also

205 estimated the correlation coefficient as well as normalized mean biases (NMB) of the
206 simulated values compared against the satellite retrieved values over two subregions.
207 Quantitatively, the NMB values over the western US (WUS) and eastern US (EUS) are 18%
208 and 7%, respectively (Figure 1C-D). In addition, the spatial variability of the 2001-2010
209 averaged annual AOD distribution (Supplementary Figure 1) is also well represented in our
210 simulation, although the model underestimates high AOD values. Similar spatial variability
211 and biases in AOD and PM_{2.5} were also found when a comparison was performed for only
212 summer months (June through August; JJA). The simulated PM_{2.5} has also been evaluated
213 against the ground-based Interagency Monitoring of Protected Visual Environments
214 (IMPROVE) data, showing similar spatial pattern and biases (10-25%) (Supplementary
215 Figure 2). The biases are smaller over Eastern US and Southwestern US region. The
216 simulated PM_{2.5} values over California matches quite well with the observed annual mean
217 values. However, the biases over Northwestern US region are ~30-40%, a portion of which
218 could be attributed to possible biases in model's meteorology in northwestern US region.
219 Nonetheless, both satellite and in situ evaluation indicate that our simulation biases are
220 largely within the uncertainty range among the various satellite and ground-based datasets,
221 which have normalized mean biases ranging from -3.3% to 33.3% when benchmarked against
222 the ground-based IMPROVE data over the contiguous US (Diao et al., 2019; Val Martin et al.
223 (2015)).

224 Discrepancies between the simulated and observed PM_{2.5} values may be attributed to
225 several potential reasons. First, the satellite-derived data has a non-zero lower bound of PM_{2.5}
226 concentrations, so the ambient background concentrations for relatively cleaner regions such
227 as the western US may be overestimated (Figure 1C), also the sampling frequency between
228 these datasets are different. Second, year 2000-based constant non-fire emissions were used
229 in the RESFire simulation, which may result in overestimation of the PM_{2.5} concentrations

230 from non-fire sources during 2001-2010 when anthropogenic emissions and PM_{2.5}
231 concentrations continue to decrease (US EPA, 2018). This overestimation is prominent in
232 regions dominated by non-fire sources such as the southeastern US. Third, large uncertainties
233 in fuel consumption and emission factors preclude an accurate estimation of the primary fire
234 emissions in the model, especially for the eastern US where large fractions of low-intensity
235 prescribed fires consume only under-canopy fuels such as litter and duff layers. The fire
236 model may fail to capture the subtle distinctions between low-intensity prescribed fires and
237 forest fires, so more fuels are consumed and result in higher emissions. Lastly, comparison of
238 a coarsely resolved simulation against in-situ observations also contributes to uncertainty.
239 Differences in the degree to which fire-climate interactions and other physical processes and
240 feedbacks are represented by the models can explain the slight differences in estimating the
241 present day mean wildfire-induced change in PM_{2.5} over local and downwind regions
242 between our simulations and previous studies. Nonetheless, reasonable simulation of the
243 spatial distribution of wildfire burnt area, AOD, and near surface particulate concentration
244 (mean bias of ~10-20 %) instills confidence about the fidelity of our model setup in
245 particulate pollution simulation, which is the focus of this study.



246

247

248 Figure 1: Comparison of the 10-year (2001-2010) averaged annual mean surface $PM_{2.5}$
 249 concentration between observations and RESFire simulations. (a) Satellite-derived surface
 250 $PM_{2.5}$ concentrations (with dust and sea-salt removed) estimated by Donkelaar et al., 2018
 251 (available at [https://sedac.ciesin.columbia.edu/data/set/sdei-global-annual-gwr-pm2-5-modis-](https://sedac.ciesin.columbia.edu/data/set/sdei-global-annual-gwr-pm2-5-modis-misr-seawifs-aod)
 252 [misr-seawifs-aod](https://sedac.ciesin.columbia.edu/data/set/sdei-global-annual-gwr-pm2-5-modis-misr-seawifs-aod); last access: 5 November, 2021); (b) 2000_{ALL} Simulated surface $PM_{2.5}$
 253 concentrations (with dust and sea-salt removed) averaged over 2001-2010; The red boxes
 254 denote the two subregions (EUS and WUS) shown in Fig. 2 in the main text. (c) comparison
 255 of simulated and satellite based gridded surface $PM_{2.5}$ concentrations in the WUS subregion;
 256 Number of samples is equal to the number of land grids ~ 450 (d) same as (c) but in the EUS
 257 subregion. Number of samples is equal to the number of land grids ~ 375 The red solid and
 258 dashed lines denote the 1:1 ratio line and $\pm 100\%$ biases, respectively. The correlation
 259 coefficients and NMB values are shown at the lower-right corner of each subplot.

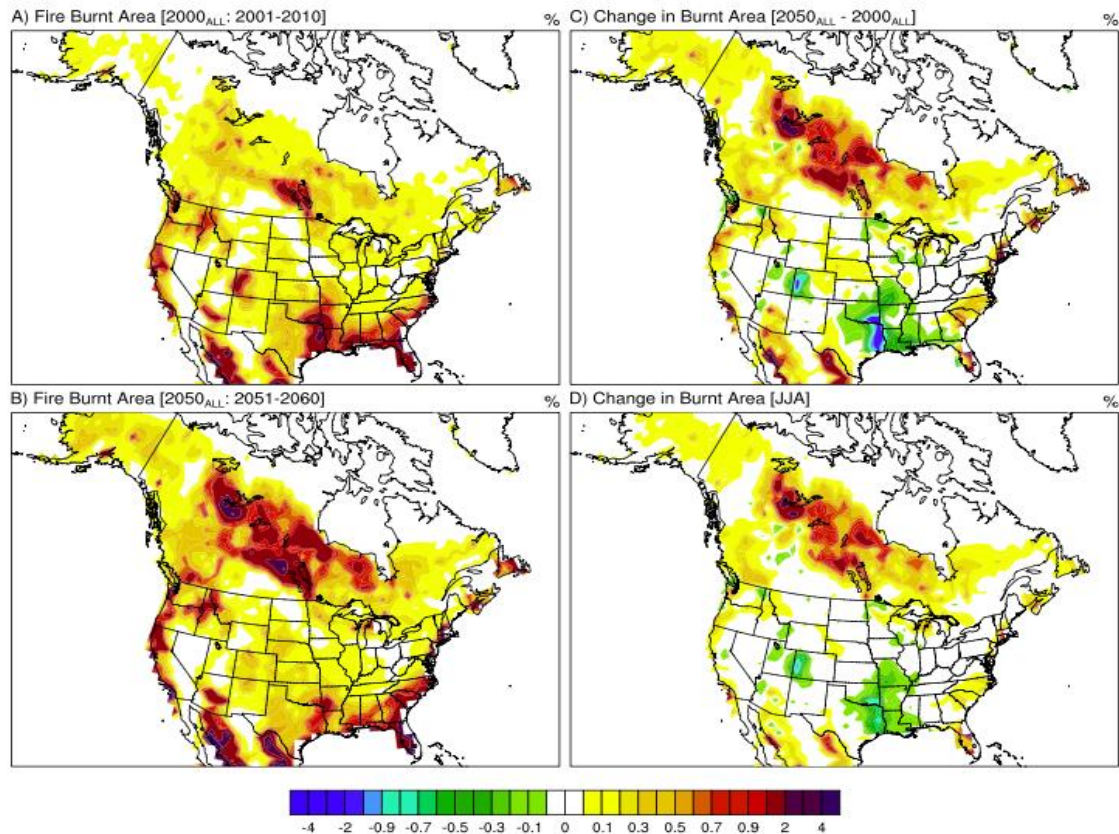
260

261 3.2 Fire-induced changes in burnt area and $PM_{2.5}$

262 The decadal-mean annual fire burnt area simulated for the present day shows
 263 widespread wildfires over the entire North America (Figure 2A). Specifically, Canada and the
 264 forested areas of the northwestern (> 36 N latitude) and southeastern (< 36 N latitude) US are
 265 most intensely affected by wildfires in the present day. By the mid-21st century, a striking

266 increase of 2-5 times in fire burnt area is projected over Canada, Alaska, the Pacific
267 Northwest and portions of the western US by the 2050s (Figure 2B). A distinct positive shift
268 in the probability density function (PDF) of annual fire burnt area is evident in the future,
269 with the decadal-mean difference statistically significant at the 99% confidence level (Zou et
270 al., 2020). A small and statistically insignificant change in interannual variability ($\sim 0.4 \text{ Mha}$
271 yr^{-1}) of fire burnt areas is also simulated between the present and future. Specifically, our
272 model predicts more than a doubling of burnt area in boreal regions of Canada in the future,
273 in line with a previous projection for Canada (Wotton et al., 2017). Future enhancement in
274 fire burnt area is $\sim 20\text{-}50\%$ in most fire grids over the western coast of US, which is higher
275 than that over the eastern US (Figures 2A and 2C). The increase over the western US is closer
276 to the lower bound of that derived from statistical model ensemble projections for the western
277 US in the mid-21st century (Yue et al., 2013). The statistics-based projections of future burnt
278 area over North America were likely too high because fire-induced land cover change, fuel
279 load reduction and factors could induce a negative fire feedback, which was not considered in
280 previous fire projection studies (Zou et al. 2020).

281 Annual fire burnt area in the southeastern US shows a decline in the future (Figure
282 2C), as precipitation is projected to increase in that region (discussed later). Note that all
283 future fire changes between 2050_{ALL} and 2000_{ALL} are primarily associated with climate
284 warming in response to the increase in greenhouse gas (GHG) concentrations in the RCP4.5
285 scenario. No direct impacts of population and socioeconomic changes on wildfires are
286 included in our simulations, although these factors contribute to changes in GHG emissions
287 (via the RCP scenario) that influence the climate simulated in 2000_{ALL} and 2050_{ALL}. As about
288 80% of the projected fire changes in the future is restricted to the summer season (June
289 through August; JJA) (Figure 2D), we focus on analysis of the summer-mean wildfire-
290 induced PM_{2.5} and its projected future changes over North America.



291

292 **Figure 2: Spatial distribution of fire burnt area.** **A-D**, Spatial distribution of simulated
 293 decadal-mean annual burnt area (as percentage) over North America for present day (A),
 294 mid-21st century (B) and the net change between the 2050s and the 2000s (C). **D**, same as
 295 (C), but for wildfire burnt area during summer only (June through August; JJA). The colorbar
 296 illustrate grid fraction of area burnt.

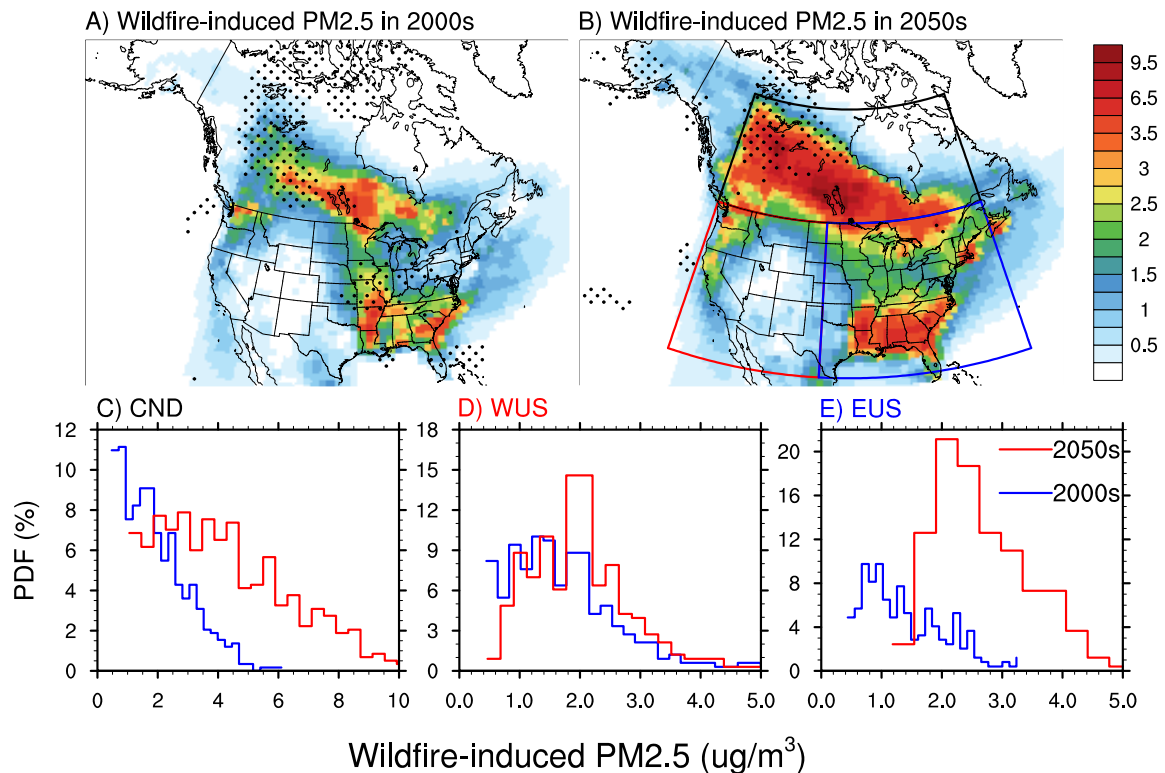
297

298

The simulated 10-year averaged summer-mean wildfire-induced PM_{2.5} values in
 299 2000_{ALL} are more than 0.5 μg/m³ over a large part of North America in the present day, with
 300 noticeably larger values (> 1 μg/m³) in Canada and the northwestern, central, and
 301 southeastern US (Figure 3A). Interestingly, the spatial distribution of wildfire-induced
 302 PM_{2.5} > 1 μg/m³ resembles an inverted horse-shoe shape. The inverted horse-shoe shaped
 303 spatial distribution is also consistent with the wildfire-smoke climatology derived from the
 304 satellite-guided operational smoke product of the Hazard Mapping System (HMS) during
 305 2005-2015 (Brey et al., 2018; Kaulfus et al., 2017). By the mid-21st century, the spatial extent
 306 of the horse-shoe shape for areas with wildfire-induced PM_{2.5} enhancement > 1 μg/m³
 307 expands significantly to span most regions of North America, with the most pronounced

308 enhancement occurring over Canada (Figure 3B). The PDFs of the spatial distribution for the
309 three regions can be seen in Figure 3C-E. Specifically, wildfire induced PM_{2.5} in the 2000s
310 over Canada, WUS and EUS during summer is ~ 1-3 μg/m³, 1-3 μg/m³ and 0.6-1.2 μg/m³,
311 respectively. Maximum values within the WUS region are found over the Pacific Northwest,
312 with most areas having wildfire induced PM_{2.5} values of ~ 2-3 μg/m³. Similarly, the southern
313 states have relatively high wildfire induced PM_{2.5} concentrations of ~ 2-4 μg/m³ within the
314 EUS in the present-day simulation.

315 Compared to the 2000s, the wildfire induced JJA-averaged PM_{2.5} values are almost
316 doubled to ~ 3-6 μg/m³ over Canada in the 2050s (Figure 3B and Figure 3C). Consistently,
317 the values of wildfire induced PM_{2.5} over WUS (mainly coastal) also doubled in 2050s
318 compared to 2000s, with modal values of ~ 2-2.5 μg/m³ (Figure 3D). Most interestingly, the
319 enhancement in wildfire-induced summer-mean PM_{2.5} over the northern EUS is also
320 significant by the 2050s (Figures 3B). Largely, the summer-mean wildfire-induced PM_{2.5}
321 concentration over EUS increases from ~0.8 to ~2 μg/m³ in the mid-century to values of 1.2-
322 3.0 μg/m³ (Figure 3E). The summer-mean wildfire-induced PM_{2.5} is thus projected to double
323 in North America by the 2050s compared to the 2000s, with a substantial coverage over the
324 EUS. An important finding from these PDFs appears to be that there are fewer grids with < 1
325 μg/m³ wildfire induced PM_{2.5}, or alternatively, that more regions are being influenced by
326 PM_{2.5}, and many areas that were already seeing wildfire impacts are seeing enhanced
327 impacts. Such enhancement is found not only at the surface but also in an elevated
328 atmospheric layer over EUS between 900 and 700 hPa. This is nonintuitive given the fact that
329 the increase in fire-burnt area by mid-century over the EUS is not substantial.



330

331 **Figure 3: Spatial distribution of PM_{2.5} concentrations.** Spatial distribution of decadal-mean
 332 wildfire-induced enhancement in summer (June through August; JJA) PM_{2.5} concentration
 333 over North America for present day (A, 2000_{ALL}-2000_{WEF}) and future (B, 2050_{ALL}-2050_{WEF}).
 334 The grids with statistical significance of 90% is identified by black dots. **C-E**, Probability
 335 density functions (PDFs) of wildfire contribution within the three regions shown in Figure 2B
 336 for Canada (CND: black box) (C), WUS (red box) (D), and EUS (blue box) (E), respectively, for
 337 2000s (blue) and 2050s (red). Only grids over land in North America are used to generate
 338 the PDFs. The y-axis indicates the probability of occurrence of different PM_{2.5} values shown
 339 in the x-axis. The colorbar illustrates PM_{2.5} in $\mu\text{g}/\text{m}^3$.

340

341 As anthropogenic- and wildfire-induced PM_{2.5} concentrations may change differently

342 with time across North America, next, we investigate the relative contribution of wildfire-

343 induced PM_{2.5} to the total PM_{2.5} in the future. Prominent enhancement of the wildfire

344 contribution is apparent in the entire domain by the 2050s (Figures 4A-B). Largely, during

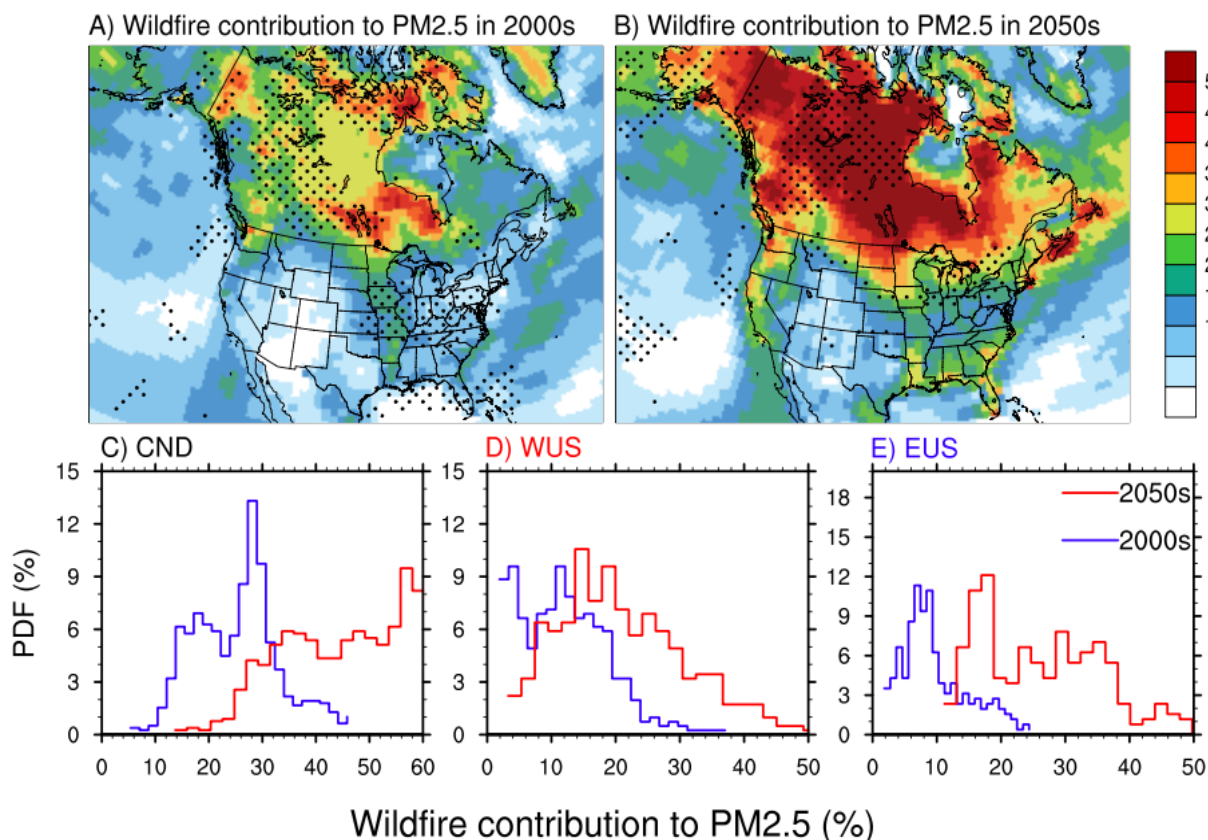
345 the 2000s, the simulated fractional contribution of wildfires to PM_{2.5} is ~15-50 % in Canada

346 (Figure 4A). Specifically, a bi-modal distribution is simulated over Canada with modal values

347 around 18% and 30% (Figure 4C). Over WUS, the present day simulated percentage

348 contributions of wildfire-induced values are 5-25% (Figure 4A), with modal values between

349 10-20% (Figure 4D). Note that many areas located in the Pacific Northwest have higher
 350 values of ~30-40% (Figure 4A). At the same time, the fractional contribution by wildfire-
 351 induced PM_{2.5} is ~5-10% in most areas of EUS in present day (Figure 4F). Nevertheless,
 352 some areas in the central US also have higher values of ~10-25% (Figure 4A).

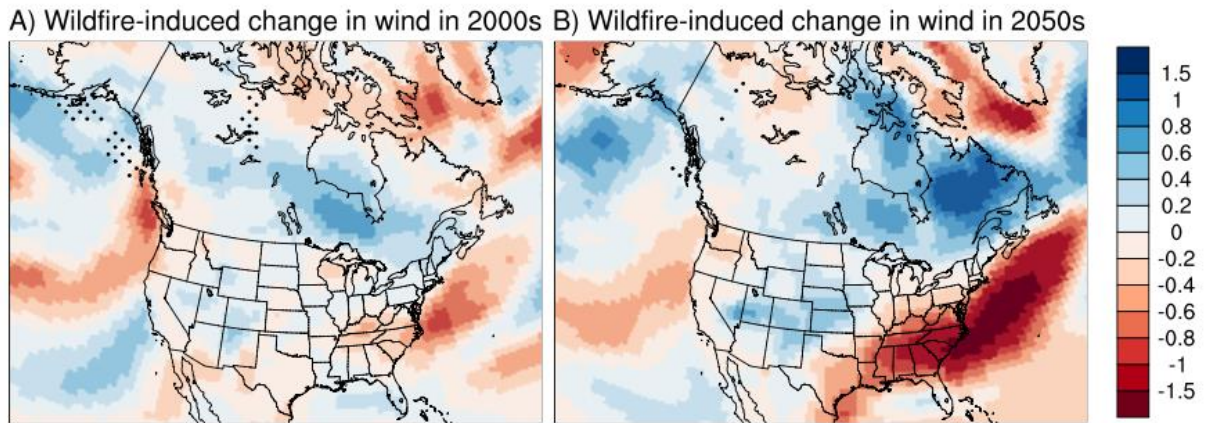


353
 354 **Figure 4: Spatial distribution and probability density function of the percentage**
 355 **contribution of wildfire emissions. A-B**, Spatial distribution of the percentage contribution
 356 of wildfire emissions to decadal-averaged summer (June through August; JJA) mean PM_{2.5}
 357 concentrations over North America during present day (A) and future (B). The percentage
 358 contribution of wildfire-induced PM_{2.5} to the total PM_{2.5} concentrations is calculated as
 359 $([2000_{ALL}-2000_{WEF}]/2000_{ALL})$ and $([2050_{ALL}-2050_{WEF}]/2050_{ALL})$ for the present and future,
 360 respectively. The grids with statistical significance of 90% is identified by black dots. **C-E**,
 361 Probability density functions (PDFs) of the percentage wildfire contribution within the three
 362 regions shown in Figure 2D for Canada (CND: black box) (C), WUS (red box) (D), and EUS
 363 (blue box) (E), respectively, for the 2000s (blue) and the 2050s (red). Only grids over land in
 364 North America are used to generate the PDFs. The y-axis indicates the probability of
 365 occurrence of different PM_{2.5} values shown in the x-axis.

367 The wildfire contributions in the 2050s show a clear shift towards higher values in all
368 sub-regions compared to the 2000s (Figure 4B). Over Canada, the values shifted from 15-30
369 % in the 2000s to ~30-60% in the 2050s, a nearly two-fold increase in the fractional
370 contribution of wildfire emissions to the total PM_{2.5} concentration is simulated (Figure 4B
371 and corresponding PDF in Figure 4C). Similarly, the contribution values increased to ~ 10-35
372 % in the 2050s, compared to 10-20% in the 2000s over WUS (Figure 4B), thereby featuring a
373 broadening of the bi-modal distribution of wildfire contribution (Figure 4D). The shift in the
374 percentage contribution is most prominent for the higher values, corresponding to some areas
375 located in the Pacific Northwest and west coast of the US (Figure 4B). Consistent with Figure
376 3B, the shift in the contribution values over EUS is also very distinct, revealing an increase in
377 the mode values from 6-10% in the 2000s to ~16-20 % by the 2050s (Figure 4B and Figure
378 4E). Thus, not only in absolute values, but our results also underscore a large increase in the
379 contribution of wildfire emissions over EUS in the future.

380 **3.3. Mechanistic understanding of the underlying processes**

381 The larger enhancement in the relative contribution of wildfire emissions to the total
382 surface PM_{2.5} in EUS in the 2050s can be explained by three mechanisms. First, due to the
383 increase in Canadian and western US wildfires, downwind transport of wildfire smoke
384 plumes to EUS will be enhanced by the 2050s. This long-range transport to the atmospheric
385 column of EUS can happen within a few days of the fire occurrence (Supplementary Figures
386 3A and 3B). Using Hazard Mapping System (HMS)-detected smoke plumes, recent studies
387 identified a strong positive association between the transported smoke plumes in the
388 atmospheric column and collocated surface PM_{2.5} enhancement in EUS (Brey et al., 2018;
389 Wu et al., 2018; Gunsch et al., 2018; Kaulfus et al., 2017; Larsen et al., 2017; Dempsey,
390 2013). Hazard Mapping System (HMS) is an operational smoke detection product over North



391

392 Figure 5a: Spatial distribution of decadal mean summer (June through August; JJA) wildfire-
 393 induced future changes $[(2050_{ALL} - 2050_{WEF}) - (2000_{ALL} - 2000_{WEF})]$. A) Wind speed below 850
 394 hpa for $[(2050_{ALL} - 2000_{ALL})]$, B) Wind speed below 850 hpa $[(2050_{WEF}) - (2000_{WEF})]$. The
 395 unit is m/s. The grids with statistical significance of 90% is identified by black dots.

396 America known as developed by the National Oceanic and Atmospheric Administration
 397 (NOAA) and operated by National Environmental Satellite, Data, and Information Service
 398 (NESDIS), available at <http://satepsanone.nesdis.noaa.gov/FIRE/fire.html>. Specifically, these
 399 studies found that the smoke plumes transported from Canada are located at an altitude of ~
 400 1-3 km over EUS (Colarco et al., 2004; Wu et al., 2018). Due to mixing by the daytime
 401 boundary layer and deposition, the smoke plumes enhance the surface PM_{2.5} concentration
 402 over EUS (Wu et al., 2018; Colarco et al., 2004; Rogers et al., 2020; Dreessen et al., 2015).
 403 Hence HMS smoky days may be a useful proxy for wildfire-induced surface PM_{2.5} over
 404 North America. In agreement, Brey et al. (2018) showed that the HMS-based smoke plumes
 405 observed over EUS is significantly aged, suggestive of their long-range transport origin.
 406 Consistent with the observed temporal change in HMS pattern, Xue et al. (2021) estimated
 407 using the mid-visible Multi Angle Implementation of Atmospheric Correction (MAIAC)
 408 satellite-derived Aerosol Optical Depth (AOD) that Canadian and western US fires have
 409 caused an increase in the daily PM_{2.5} over Montana, North Dakota, South Dakota and
 410 Minnesota by 18.3, 12.8, 10.4 and 10.1 $\mu g m^{-3}$, respectively, between August 2011 (a low
 411 fire month) and August 2018 (a high fire month). In summary, the visually apparent satellite-

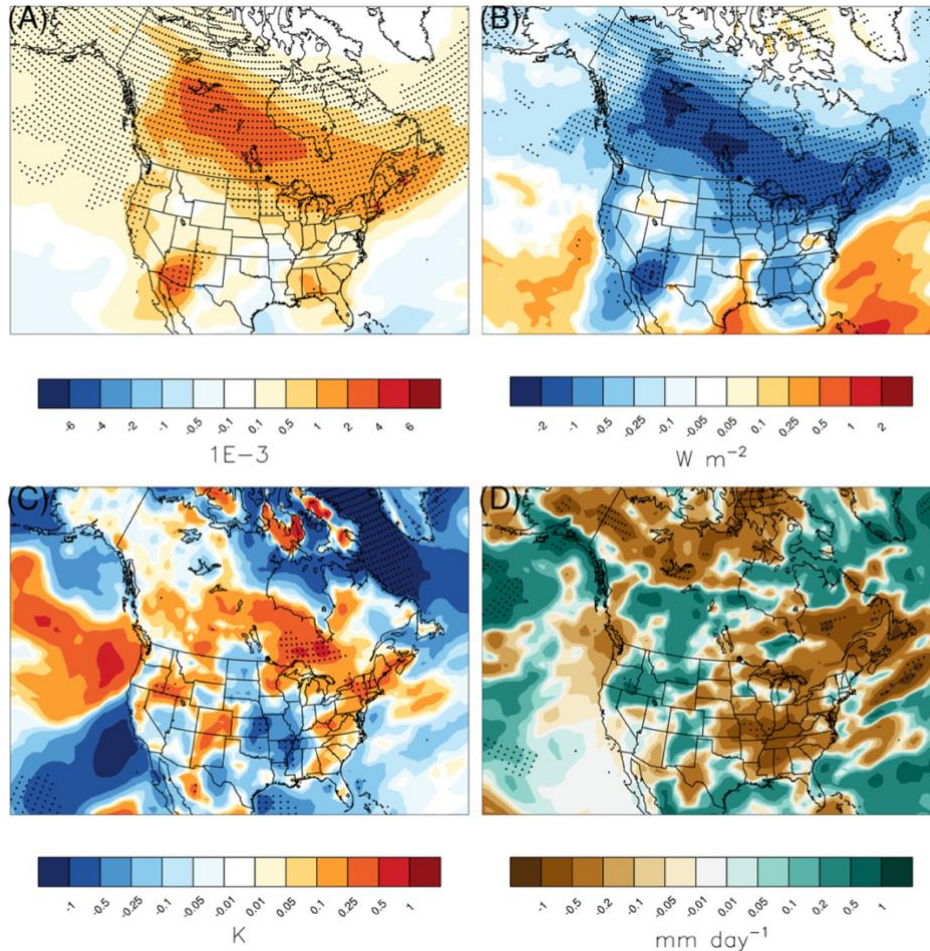
412 based signatures of wildfire-smoke across Canada and EUS provide a necessary, though not
413 sufficient, support for the influence of Canadian smoke plumes on EUS air quality. Although,
414 the change in burnt area over northeastern EUS is negligible compared to the western US and
415 Canadian regions, however, there are some enhancements seen over east coast of US, which
416 can also contribute to enhanced fire emissions.

417 In future, the wildfire-induced change in speed of the westerly jet flows over Canada
418 wildfire regions is increased (Figure 5 A-B). It indicates that the westerly-induced transported
419 wildfire emissions from Canada boreal forests to the eastern half of Northern America and
420 EUS will be enhanced in future compared to that in present era. On the one hand, the
421 wildfire-induced changes in wind speed over the EUS is reduced in future, which implies that
422 the local emissions over EUS are less dispersed. Simultaneously, this will also cause the
423 transporting smoke plumes to slow down and be subjected to relatively more boundary layer
424 mixing over the EUS and dry deposition/settling enhances, thereby contributing to the
425 enhanced PM_{2.5} values at surface. The westerly winds over western US below 40° N is also
426 strengthened in future (Figure 5 A-B) compared to present day which indicates more
427 advection flux wildfire emissions to EUS. Thus, the net effect is more removal of wildfire-
428 emitted PM_{2.5} from WUS and more influx of wildfire-emitted PM_{2.5} in EUS.

429 Along with this dynamical changes, other climatic feedbacks simulated can also contribute to
430 enhancement of EUS pollution. Specifically, the enhancement of wildfire-induced smoke
431 aerosols increases solar absorption and scattering in the future (Figure 6A). This reduces the
432 incoming solar radiation reaching at the surface (Figure 6B) and induces surface cooling.
433 With atmospheric warming and surface cooling, lower-tropospheric stability is enhanced by
434 wildfire aerosols in the future (Figure 6C). The smoke plumes which reaches eastern US are
435 at an elevated altitude due to self-lofting property of absorbing aerosols as they travel

436 downwind but the smoke over western US is at near surface elevation as it is at its source
437 region. This can explain the more significant atmospheric stability simulated over the eastern
438 US compared to the source regions in western US and boreal forests of Canada. Relatively
439 stronger atmospheric stability over eastern US impose a stronger thermal capping that traps
440 more anthropogenic aerosols and particulate matter near the surface over EUS (already an
441 emission hotspot). At the same time, future increase in wildfire emissions also leads to
442 greater reduction of monthly rainfall (Figure 6D) over EUS, which may additionally
443 strengthen the positive feedback to surface PM_{2.5} over EUS by reducing wet scavenging of
444 transported wildfire smoke to EUS. Thus, wildfire-emitted aerosols induce positive feedback
445 on the surface PM_{2.5} concentration over EUS through fire-climate interactions that vary on a
446 regional scale. Moreover, the above discussed dynamical changes in future can also feedback
447 these simulated thermodynamical and precipitation changes, exaggerating the enhancement in
448 PM_{2.5} values over EUS in future. However, due to computational constrains, no direct
449 quantification of the magnitude of these feedback (with aerosol-radiation and aerosol-cloud
450 interactions turned off) on PM_{2.5} is performed and would be taken up in future studies.

451 Lastly, the reason of why the contribution of wildfire emissions to the total surface
452 PM_{2.5} in EUS is so substantial in the 2050s is the drastic reduction of anthropogenic
453 contribution to the surface PM_{2.5} over EUS in the future primarily due to policy-driven
454 reduction in anthropogenic emissions under the RCP4.5 scenario. Specifically, the simulated
455 ambient summer mean PM_{2.5} concentration exhibits widespread declines in the future
456 (Supplementary Figure 4), with reduction in PM_{2.5} concentration over eastern US in the range
457 of 4-15 $\mu\text{g}/\text{m}^3$, which is greatest within North America. Thus, large reduction in
458 anthropogenic contribution combined with increased downwind advection of Canadian
459 smoke and WUS to EUS and the associated positive feedbacks can explain the projected
460 dominance of wildfire emissions over EUS in future.



461

462 Figure 6: Spatial distribution of decadal mean summer (June through August; JJA) wildfire-
 463 induced future changes $[(2050_{ALL}-2050_{WEF}) - (2000_{ALL}-2000_{WEF})]$. A) aerosol absorption
 464 optical depth at 550 nm, B) aerosol direct radiative forcing at surface, C) lower-tropospheric
 465 stability calculated as the difference between the potential temperature at 900 hPa and 1000
 466 hPa, D) summer averaged precipitation rates, over North America. Areas marked with black
 467 dots indicate grids where changes are significant at the 95% confidence level.

468

469 3.4 Future Implications and uncertainties

470

471

472

473

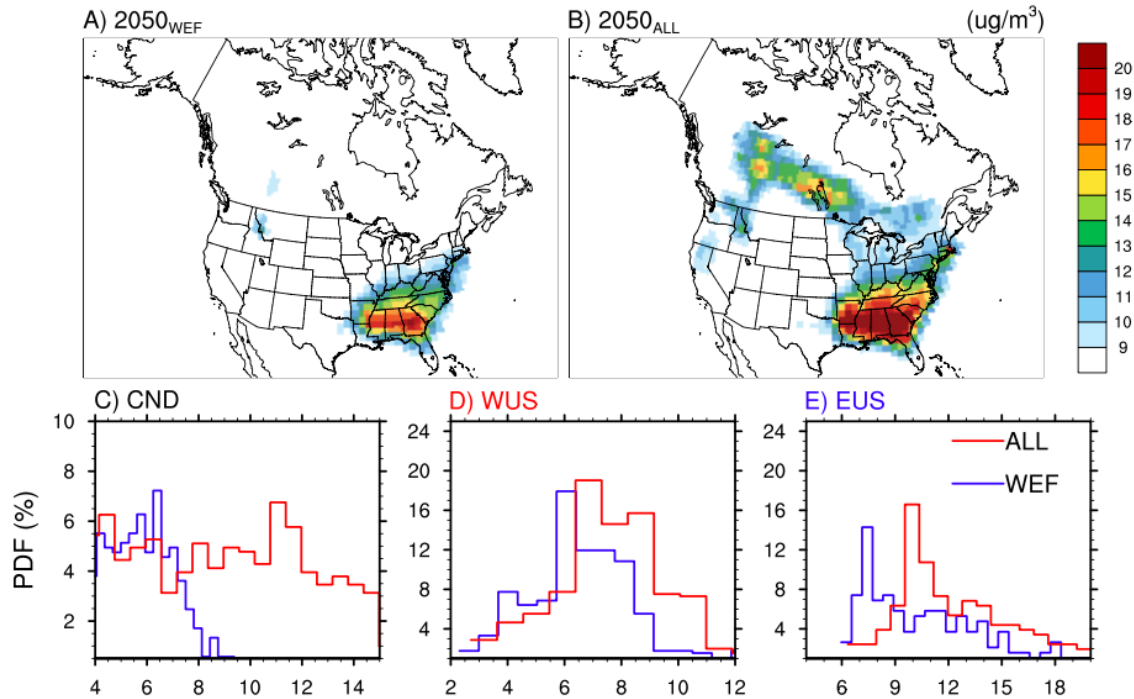
474

475

However, is the simulated future enhancement in wildfire contribution over EUS
 substantial enough to affect the surface PM_{2.5} values over EUS in future? The World Health
 Organization (WHO) air quality guidelines for annual and daily PM_{2.5} concentration are 10
 $\mu\text{g m}^{-3}$ and 25 $\mu\text{g m}^{-3}$, respectively. As no specific guideline for seasonal-mean PM_{2.5} in the
 summer is available, we use the annual guideline value as a reference to understand the
 implication of wildfire emissions on ambient PM_{2.5} concentration in the future. Interestingly,

476 the mean summertime PM_{2.5} concentration in the wildfire emission free (WEF) scenario is
477 projected to remain within 10 µg m⁻³ over most of North America, except for the
478 southeastern US (~15% of the domain) (Figure 7A). However, the ALL-scenario projects an
479 increase in the exposure concentration level such that values > 10 µg/m³ are common in
480 Canada and EUS in the future (Figure 7B). Quantitatively, over Canada, the entire PDF of
481 PM_{2.5} concentration shifts towards higher values by ~5-6 µg/m³. Specifically, the modal value
482 shifts from ~ 6 µg/m³ in 2050_{WEF} to 11-12 µg/m³ in 2050_{ALL} (Figure 7C), so PM_{2.5}
483 concentration is projected to surpass the WHO guidelines over a large fraction of Canada in
484 the future. Similarly, the entire PDF of PM_{2.5} concentration shifts towards higher values by
485 ~2-3 µg/m³ over EUS, with the mode of the PDF increasing from ~ 7-8 µg/m³ in 2050_{WEF} to
486 ~ 10-11 µg/m³ in 2050_{ALL} (Figure 7E). The modal value of summer mean PM_{2.5} over WUS
487 increases from ~ 6 µg/m³ in 2050_{WEF} to ~ 7-8 µg/m³ in 2050_{ALL} (Figure 7D), although a few
488 grid cells show PM_{2.5} values greater than 10 µg/m³ (Figure 7B).

489 Clearly, the climate-induced enhancement in fires and its influence via the advected
490 wildfire smoke to EUS can have significant implications for air quality management in the
491 future. The PM_{2.5} enhancement in future over the southern states within EUS is large (Figure
492 7A-B), which is consistent with Figure 3 and 4 results. However, the future change in burnt
493 area over the same region is negligible or mostly reducing (Figure 1C-D). Thus, it can be
494 argued that the simulated enhancement is mostly related with the dynamic perturbations and
495 thermodynamical feedbacks due to wildfire emissions (Figure 6). As the rate of
496 anthropogenic emissions is also regionally highest over the Southeastern states, the impact of
497 these wildfire-induced climatic feedbacks on local air quality is distinctly seen over the EUS.



498

499 **Figure 7: Spatial distribution and probability density function of PM_{2.5} concentration in**
 500 **2050s. A-B**, Spatial distribution of decadal-average summer (June through August; JJA)
 501 mean PM_{2.5} concentration over North America in mid-21st century from 2050_{WEF} (wildfire
 502 emission-free) (A) and 2050_{ALL} (wildfire emission-inclusive) (B). **C-E**, Probability density
 503 functions (PDFs) of the same within the three regions shown in Figure 2B for Canada; CND
 504 (C), western US; WUS (D), and eastern US; EUS (E), respectively, for the 2050_{WEF} (blue)
 505 and 2050_{ALL} (red) runs. The y-axis indicates the probability of occurrence of different PM_{2.5}
 506 values shown in the x-axis. Only grids over land in North America are used to generate the
 507 PDFs. Note the different ranges of values shown in the y- and x-axis in **C-E**. The colorbar
 508 and the x-axis for Panel C-E indicates PM_{2.5} values.

509 Note that our simulated present-day estimates of wildfire induced PM_{2.5} values as well
 510 as the percentage contribution of wildfire emissions are within the range of reported values in
 511 previous studies over the domain, which augment the fidelity our future projections.

512 Specifically, our simulated present-day estimates of wildfire induced PM_{2.5} values are also
 513 within the range of reported values in previous studies over the domain. Reported values of
 514 wildfire-induced PM_{2.5} over WUS during summertime vary from $\sim 1 \mu\text{g}/\text{m}^3$ (Jaffe et al., 2008)
 515 to $\sim 2 \mu\text{g}/\text{m}^3$ (Park et al., 2007) and $\sim 3 \mu\text{g}/\text{m}^3$ (Ford et al., 2018), with the highest values
 516 documented over the Pacific Northwest and west coast regions ($\sim 1-4 \mu\text{g}/\text{m}^3$) (O'Dell et al.,
 517 2019). The wildfire-induced PM_{2.5} over EUS during summertime varies from $\sim 1 \mu\text{g}/\text{m}^3$ (Park

518 et al., 2007) to $\sim 2.5 \mu\text{g}/\text{m}^3$ ($\sim 3 \mu\text{g}/\text{m}^3$ in the southeastern US) (Ford et al., 2018).
519 Consistently, our simulated present-day estimates of wildfire contribution values are also
520 within the range of reported values in previous studies. For example, Meng et al. (2019)
521 found that wildfires can be the largest sectoral contributor ($\sim 18\text{-}59\%$) to the population-
522 weighted $\text{PM}_{2.5}$ in various subregions of Canada. Over WUS, the present-day percentage
523 contribution of wildfire induced $\text{PM}_{2.5}$ to the total $\text{PM}_{2.5}$ is reported to be $\sim 12\%$ (Liu et al.,
524 2017), $\sim 15\%$ (Park et al., 2007) and $\sim 30\%$ (Ford et al., 2018), with higher values of $\sim 40\%$ in
525 the Pacific Northwest (O'Dell et al., 2019). Over EUS our simulated values are also within
526 the range of previously reported values of $\sim 5\%$ (Park et al., 2007) and $\sim 15\text{-}18\%$ (Ford et al.,
527 2018). However, our two-way coupled simulations illustrate that future enhancement in the
528 wildfire associated $\text{PM}_{2.5}$ over the EUS could be greater compared to the western US, which
529 is not emphasized explicitly in any of the previous studies (although Ford et al., 2018
530 illustrated increase in $\text{PM}_{2.5}$ over mid and central US from Canadian fires). These could be
531 since inclusion of the wildfire-induced climatic feedbacks in our simulation is an
532 unprecedented exercise. Please also note that our study is focused on JJA period and the
533 wildfires in western US mainly occurs during August-September months, so the results
534 should be compared consciously.

535 Nonetheless, inherent limitations in our simulations may introduce uncertainties in the
536 projected future changes. For example, our reported changes in $\text{PM}_{2.5}$ concentrations based on
537 relatively coarse resolution simulations and decadal averages likely represent a low-end
538 estimate compared to changes at regional and daily/weekly scales. Moreover, our
539 experiments do not consider the direct human influences such as population change and
540 socioeconomic development on wildfires, which may aggravate the increase in $\text{PM}_{2.5}$
541 concentrations over the densely populated EUS in the future. Common sources of uncertainty
542 in modeling burnt area and fire emission and fire aerosol and smoke are also present in our

543 model. Fire smoke, in particular, is extremely hard to measure and evaluate. Lastly, inherent
544 uncertainties in the physics parameterizations used in the model, sensitivity of climate to
545 GHGs emissions, and the RCP scenarios should also be noted. Thus, ensemble modeling
546 considering different emissions scenarios, population and future time periods, and the use of
547 a finer spatial resolution may provide a more robust and better quantification of the wildfire-
548 induced impact on policy regulated improvements in PM_{2.5} over EUS.

549 **4. Conclusion**

550 In summary, online coupled fire-climate-ecosystem simulations project a nearly
551 twofold increase in wildfire-induced summer-mean surface PM_{2.5} concentration by the mid-
552 21st century over the entire North America. In a wildfire-emission free future, a large portion
553 of North America will have PM_{2.5} values below the WHO guidelines. But in a future with
554 wildfire emissions, the improvements from policy-driven reductions in anthropogenic PM_{2.5}
555 will be compromised by the projected doubling of PM_{2.5} from wildfires. More strikingly,
556 wildfire-induced enhancement in surface PM_{2.5} values and percentage contribution of the
557 wildfire emissions over EUS could be substantial by mid-century. This is mainly because of
558 the large enhancement in fires over Northern America by 2050s and associated increase in
559 amount of downwind transport of smoke to EUS. In addition, enhancement of smoke
560 transport induces a positive climate feedback to PM_{2.5} concentrations over EUS by increasing
561 the lower-tropospheric stability and reducing wet scavenging rates. Despite the inherent
562 limitations, this study highlights the natural versus anthropogenic contributions and the non-
563 local nature of air pollution that can complicate regulatory strategies aimed at improving air
564 quality over the eastern US in a warmer future.

565

566

567 **Data availability statements**

568 The HMS data used in this paper are available free through the link
569 <https://www.ospo.noaa.gov/Products/land/hms.html>. The model simulations data are
570 available at <https://portal.nersc.gov/project/m1660/yang560/wildfire>

571 **Code availability statements**

572 The model code and scripts are available at
573 <https://portal.nersc.gov/project/m1660/yang560/wildfire>

574

575 **Acknowledgements:**

576 This research was performed at PNNL and funded under Assistance Agreement No.
577 RD835871 by the U.S. Environmental Protection Agency to Yale University through the
578 SEARCH (Solutions for Energy, AiR, Climate, and Health) Center. It has not been formally
579 reviewed by EPA. The views expressed in this document are solely those of the SEARCH
580 Center and do not necessarily reflect those of the Agency. EPA does not endorse any
581 products or commercial services mentioned in this publication. CS is supported by the New
582 Faculty Initiation Grant project number CE/20-21/065/NFIG/008961 from IIT Madras.
583 PNNL is operated by Battelle Memorial Institute for the U.S. Department of Energy under
584 contract DE-AC06-76RLO-1830.

585

586 **Authors Contribution**

587 YQ, CS and RL designed this study. CS did the model and satellite analysis and wrote the
588 first draft of the manuscript. YZou performed the simulations. All authors provided inputs
589 throughout the study and helped in the drafting and submission process.

590

591 **References**

592 Abatzoglou, J. T. and Williams, A. P.: Impact of anthropogenic climate change on wildfire
593 across western US forests, *Proc. Natl. Acad. Sci.*, 113(42), 11770 LP – 11775,
594 doi:10.1073/pnas.1607171113, 2016.

595 Andela, N., Morton, D. C., Giglio, L., Chen, Y., van der Werf, G. R., Kasibhatla, P. S.,
596 DeFries, R. S., Collatz, G. J., Hantson, S., Kloster, S., Bachelet, D., Forrest, M., Lasslop, G.,
597 Li, F., Mangeon, S., Melton, J. R., Yue, C. and Randerson, J. T.: A human-driven decline in
598 global burned area, *Science* (80-.), 356(6345), 1356 LP – 1362,
599 doi:10.1126/science.aal4108, 2017.

600 Anjali, H., Muhammad, A., Anthony, D. M., Karen, S., R., S. M., Mick, M., M., T. A., J., A.
601 M. and Martine, D.: Impact of Fine Particulate Matter (PM_{2.5}) Exposure During Wildfires on
602 Cardiovascular Health Outcomes, *J. Am. Heart Assoc.*, 4(7), e001653,
603 doi:10.1161/JAHA.114.001653, 2019.

604 Black, C., Tesfaigzi, Y., Bassein, J. A. and Miller, L. A.: Wildfire smoke exposure and
605 human health: Significant gaps in research for a growing public health issue, *Environ.*

606 Toxicol. Pharmacol., 55, 186–195, doi:<https://doi.org/10.1016/j.etap.2017.08.022>, 2017.

607 Brey, S. J., Ruminski, M., Atwood, S. A. and Fischer, E. V: Connecting smoke plumes to
608 sources using Hazard Mapping System (HMS) smoke and fire location data over North
609 America, Atmos. Chem. Phys., 18(3), 1745–1761, doi:10.5194/acp-18-1745-2018, 2018.

610 Dempsey, F.: Forest Fire Effects on Air Quality in Ontario: Evaluation of Several Recent
611 Examples, Bull. Am. Meteorol. Soc., 94(7), 1059–1064, doi:10.1175/BAMS-D-11-00202.1,
612 2013.

613 Dominici, F., Peng, R. D., Bell, M. L., Pham, L., McDermott, A., Zeger, S. L. and Samet, J.
614 M.: Fine Particulate Air Pollution and Hospital Admission for Cardiovascular and
615 Respiratory Diseases, JAMA, 295(10), 1127–1134, doi:10.1001/jama.295.10.1127, 2006.

616 Diao, M., Holloway, T., Choi, S., O’Neill, S.M., Al-Hamdan, M.Z., Van Donkelaar, A.,
617 Martin, R.V., Jin, X., Fiore, A.M., Henze, D.K. and Lacey, F., 2019. Methods, availability,
618 and applications of PM_{2.5} exposure estimates derived from ground measurements, satellite,
619 and atmospheric models. *Journal of the Air & Waste Management Association*, 69(12),
620 pp.1391-1414.

621 Ford, B., Val Martin, M., Zelasky, S. E., Fischer, E. V, Anenberg, S. C., Heald, C. L. and
622 Pierce, J. R.: Future Fire Impacts on Smoke Concentrations, Visibility, and Health in the
623 Contiguous United States, GeoHealth, 2(8), 229–247, doi:10.1029/2018GH000144, 2018.

624 Gillett, N. P., Weaver, A. J., Zwiers, F. W. and Flannigan, M. D.: Detecting the effect of
625 climate change on Canadian forest fires, Geophys. Res. Lett., 31(18),
626 doi:10.1029/2004GL020876, 2004.

627 Gunsch, M. J., May, N. W., Wen, M., Bottenus, C. L. H., Gardner, D. J., VanReken, T. M.,
628 Bertman, S. B., Hopke, P. K., Ault, A. P. and Pratt, K. A.: Ubiquitous influence of wildfire
629 emissions and secondary organic aerosol on summertime atmospheric aerosol in the forested
630 Great Lakes region, Atmos. Chem. Phys., 18(5), 3701–3715, doi:10.5194/acp-18-3701-2018,
631 2018.

632 Guan S, Wong DC, Gao Y, Zhang T, Pouliot G. Impact of wildfire on particulate matter in
633 the southeastern United States in November 2016. *Sci Total Environ.* 2020;724:138354.
634 doi:10.1016/j.scitotenv.2020.138354.

635 Johnston F. H., Henderson. S. B., Yang, C., T., R. J., Miriam, M., S., D. R., Patrick, K.,
636 M.J.S., B. D. and Michael, B.: Estimated Global Mortality Attributable to Smoke from
637 Landscape Fires, Environ. Health Perspect., 120(5), 695–701, doi:10.1289/ehp.1104422,
638 2012.

639 Harris, R. M. B., Remenyi, T. A., Williamson, G. J., Bindoff, N. L., and Bowman, D. M. J.
640 S.: Climate-vegetation fire interactions and feedbacks: trivial detail or major barrier to
641 projecting the future of the Earth system?, *Wires Clim. Change*, 7, 910-931,
642 10.1002/wcc.428, 2016.

643 Hantson, S., Arneth, A., Harrison, S. P., Kelley, D. I., Prentice, I. C., Rabin, S. S., et al.
644 (2016). The status and challenge of global fire modelling. *Biogeosciences*, 13, 3359–3375.
645 <https://doi.org/10.5194/bg-13-3359-2016>

646 Hu, X., Yu, C., Tian, D., Ruminski, M., Robertson, K., Waller, L. A. and Liu, Y.:
647 Comparison of the Hazard Mapping System (HMS) fire product to ground-based fire records

648 in Georgia, USA, *J. Geophys. Res. Atmos.*, 121(6), 2901–2910, doi:10.1002/2015JD024448,
649 2016.

650 HURTT, G. C., FROLKING, S., FEARON, M. G., MOORE, B., SHEVLIAKOVA, E.,
651 MALYSHEV, S., PACALA, S. W. and HOUGHTON, R. A.: The underpinnings of land-use
652 history: three centuries of global gridded land-use transitions, wood-harvest activity, and
653 resulting secondary lands, *Glob. Chang. Biol.*, 12(7), 1208–1229, doi:10.1111/j.1365-
654 2486.2006.01150.x, 2006.

655 Jaffe, D., Hafner, W., Chand, D., Westerling, A. and Spracklen, D.: Interannual Variations in
656 PM_{2.5} due to Wildfires in the Western United States, *Environ. Sci. Technol.*, 42(8), 2812–
657 2818, doi:10.1021/es702755v, 2008.

658 Jolly, W. M., Cochrane, M. A., Freeborn, P. H., Holden, Z. A., Brown, T. J., Williamson, G.
659 J. and Bowman, D. M. J. S.: Climate-induced variations in global wildfire danger from 1979
660 to 2013, *Nat. Commun.*, 6, 7537 [online] Available from:
661 <https://doi.org/10.1038/ncomms8537>, 2015.

662 Kaulfus, A. S., Nair, U., Jaffe, D., Christopher, S. A. and Goodrick, S.: Biomass Burning
663 Smoke Climatology of the United States: Implications for Particulate Matter Air Quality,
664 *Environ. Sci. Technol.*, 51(20), 11731–11741, doi:10.1021/acs.est.7b03292, 2017.

665 Kirchmeier-Young, M. C., Zwiers, F. W., Gillett, N. P. and Cannon, A. J.: Attributing
666 extreme fire risk in Western Canada to human emissions, *Clim. Change*, 144(2), 365–379,
667 doi:10.1007/s10584-017-2030-0, 2017.

668 Kitzberger, T., Falk, D. A., Westerling, A. L. and Swetnam, T. W.: Direct and indirect
669 climate controls predict heterogeneous early-mid 21st century wildfire burned area across
670 western and North America, *PLoS One*, 12(12), e0188486 [online] Available from:
671 <https://doi.org/10.1371/journal.pone.0188486>, 2017.

672 Knorr, W., Dentener, F., Lamarque, J.-F., Jiang, L. and Arneth, A.: Wildfire air pollution
673 hazard during the 21st century, *Atmos. Chem. Phys.*, 17(14), 9223–9236, doi:10.5194/acp-
674 17-9223-2017, 2017.

675 Koplitz, S.N., Nolte, C.G., Pouliot, G.A., Vukovich, J.M. and Beidler, J., 2018. Influence of
676 uncertainties in burned area estimates on modeled wildland fire PM_{2.5} and ozone pollution
677 in the contiguous US. *Atmospheric environment*, 191, pp.328-339.

678 Lamarque, J. F., Bond, T. C., Eyring, V., Granier, C., Heil, A., Klimont, Z., Lee, D., Liousse,
679 C., Mieville, A., Owen, 628 B., Schultz, M. G., Shindell, D., Smith, S. J., Stehfest, E., Van
680 Aardenne, J., Cooper, O. R., Kainuma, M., 629 Mahowald, N., McConnell, J. R., Naik, V.,
681 Riahi, K., and van Vuuren, D. P.: Historical (1850-2000) gridded anthropogenic and biomass
682 burning emissions of reactive gases and aerosols: methodology and application, 631 *Atmos.*
683 *Chem. Phys.*, 10, 7017-7039, 10.5194/acp-10-7017-2010, 2010.

684 Leibensperger, E. M., Mickley, L. J., Jacob, D. J., Chen, W.-T., Seinfeld, J. H., Nenes, A.,
685 Adams, P. J., Streets, D. G., Kumar, N. and Rind, D.: Climatic effects of 1950–2050
686 changes in US anthropogenic aerosols – Part 2: Climate response, *Atmos. Chem.*
687 *Phys.*, 12(7), 3349–3362, doi:10.5194/acp-12-3349-2012, 2012.

688 Li, F., Zeng, X. D., & Levis, S. (2012). A process-based fire parameterization of intermediate
689 complexity in a dynamic global vegetation model. *Biogeosciences*, 9(7), 2761–2780.
690 <https://doi.org/10.5194/bg-9-2761-2012>

691 Liu, J. C., Mickley, L. J., Sulprizio, M. P., Dominici, F., Yue, X., Ebisu, K., Anderson, G. B.,
692 Khan, R. F. A., Bravo, M. A. and Bell, M. L.: Particulate Air Pollution from Wildfires in the
693 Western US under Climate Change, *Clim. Change*, 138(3), 655–666, doi:10.1007/s10584-
694 016-1762-6, 2016.

695 Liu, Y., Goodrick, S. and Heilman, W.: Wildland fire emissions, carbon, and climate:
696 Wildfire–climate interactions, *For. Ecol. Manage.*, 317, 80–96,
697 doi:https://doi.org/10.1016/j.foreco.2013.02.020, 2014.

698 Liu, X., Easter, R. C., Ghan, S. J., Zaveri, R., Rasch, P., Shi, X., Lamarque, J. F., Gettelman,
699 A., Morrison, H., Vitt, F., Conley, A., Park, S., Neale, R., Hannay, C., Ekman, A. M. L.,
700 Hess, P., Mahowald, N., Collins, W., Iacono, M. J., Bretherton, C. S., Flanner, M. G., and
701 Mitchell, D.: Toward a minimal representation of aerosols in climate models: description and
702 evaluation in the Community Atmosphere Model CAM5, *Geosci. Model Dev.*, 5, 709- 652
703 739, 10.5194/gmd-5-709-2012, 2012.

704 Meng, J., Martin, R.V., Li, C., van Donkelaar, A., Tzompa-Sosa, Z.A., Yue, X., Xu, J.W.,
705 Weagle, C.L. and Burnett, R.T., 2019. Source Contributions to Ambient Fine Particulate
706 Matter for Canada. *Environmental science & technology*, 53(17), pp.10269-10278.

707 McClure, C. D. and Jaffe, D. A.: US particulate matter air quality improves except in
708 wildfire-prone areas, *Proc. Natl. Acad. Sci.*, 115(31), 7901 LP – 7906,
709 doi:10.1073/pnas.1804353115, 2018.

710 Neale, R. B., Chen, C. C., Gettelman, A., Lauritzen, P. H., Park, S., Williamson, D. L.,
711 Conley, A. J., Garcia, R., Kinnison, D., Lamarque, J. F., Marsh, D., Mills, M., Smith, A. K.,
712 Tilmes, S., Vitt, F., Morrison, H., Cameron 671 Smith, P., Collins, W. D., Iacono, M. J.,
713 Easter, R. C., Ghan, S. J., Liu, X. H., Rasch, P. J., and Taylor, M. A.: Description of the
714 NCAR Community Atmosphere Model (CAM 5.0), NCAR 289, 2013

715 Nolte, C. G., Spero, T. L., Bowden, J. H., Mallard, M. S. and Dolwick, P. D.: The potential
716 effects of climate change on air quality across the conterminous US at 2030 under three
717 Representative Concentration Pathways, *Atmos. Chem. Phys.*, 18(20), 15471–15489,
718 doi:10.5194/acp-18-15471-2018, 2018.

719 Katelyn O’Dell, Bonne Ford, Emily V. Fischer, and Jeffrey R. Pierce *Environmental Science*
720 & *Technology* 2019 53 (4), 1797-1804, DOI: 10.1021/acs.est.8b05430.
721

722 Partain, J. L., Alden, S., Strader, H., Bhatt, U. S., Bieniek, P. A., Brettschneider, B. R.,
723 Walsh, J. E., Lader, R. T., Olsson, P. Q., Rupp, T. S., Thoman, R. L., York, A. D. and Ziel,
724 R. H.: An Assessment of the Role of Anthropogenic Climate Change in the Alaska Fire
725 Season of 2015, *Bull. Am. Meteorol. Soc.*, 97(12), S14–S18, doi:10.1175/BAMS-D-16-
726 0149.1, 2016.

727 Park, S., Bretherton, C. S., and Rasch, P. J.: Integrating Cloud Processes in the Community
728 Atmosphere Model, Version 5, *J. Climate*, 27, 6821-6856, 10.1175/Jcli-D-14-00087.1, 2014.

729 Park, R.J., Jacob, D.J. and Logan, J.A., 2007. Fire and biofuel contributions to annual mean
730 aerosol mass concentrations in the United States. *Atmospheric Environment*, 41(35), pp.7389-
731 7400.

732 Pierce, J. R., Val Martin, M., & Heald, C. L. (2017). Estimating the Effects of Changing
733 Climate on Fires and Consequences for U.S. Air Quality, Using a Set of Global and Regional
734 Climate Models (final report no. JFSP-13-1-01-4). Retrieved from

735 https://www.firescience.gov/projects/13-1-01-4/project/13-1-01-4_final_report.pdf

736 Pouliot G, Pace TG, Roy B, Pierce T, Mobley D. Development of a biomass burning
737 emissions inventory by combining satellite and ground-based information. *J Appl Remote*
738 *Sens.* 2008;2:021501. doi: 10.1117/1.2939551.

739 Randerson, J. T., Chen, Y., van der Werf, G. R., Rogers, B. M., & Morton, D. C. (2012).
740 Global burned area and biomass burning emissions from small fires. *Journal of Geophysical*
741 *Research*, 117, G04012. <https://doi.org/10.1029/2012JG002128>

742 Rolph, G. D., Draxler, R. R., Stein, A. F., Taylor, A., Ruminski, M. G., Kondragunta, S.,
743 Zeng, J., Huang, H.-C., Manikin, G., McQueen, J. T. and Davidson, P. M.: Description and
744 Verification of the NOAA Smoke Forecasting System: The 2007 Fire Season, *Weather*
745 *Forecast.*, 24(2), 361–378, doi:10.1175/2008WAF2222165.1, 2009.

746 Spracklen, D. V., Mickley, L. J., Logan, J. A., Hudman, R. C., Yevich, R., Flannigan, M. D.,
747 & Westerling, A. L. (2009). Impacts of climate change from 2000 to 2050 on wildfire activity
748 and carbonaceous aerosol concentrations in the western United States. *Journal of Geophysical*
749 *Research*, 114, D20301. <https://doi.org/10.1029/2008JD010966>

750 Sun, Y., Gu, L. H., and Dickinson, R. E.: A numerical issue in calculating the coupled carbon
751 and water fluxes in a climate model, *J. Geophys. Res.-Atmos.*, 117,
752 D2210310.1029/2012jd018059, 2012

753 Sofiev, M., Ermakova, T., and Vankevich, R.: Evaluation of the smoke-injection height from
754 wild-land fires using remote-sensing data, *Atmos. Chem. Phys.*, 12, 1995-2006, 10.5194/acp-
755 12-1995-2012, 2012

756 Shi, H., Jiang, Z., Zhao, B., Li, Z., Chen, Y., Gu, Y., Jiang, J. H., Lee, M., Liou, K.-N., Neu,
757 J. L., Payne, V. H., Su, H., Wang, Y., Witek, M. and Worden, J.: Modeling Study of the Air
758 Quality Impact of Record-Breaking Southern California Wildfires in December 2017, *J.*
759 *Geophys. Res. Atmos.*, 0(0), doi:10.1029/2019JD030472, 2019.

760 U.S. EPA (U.S. Environmental Protection Agency). 2009. Integrated Science Assessment
761 (ISA) For Particulate Matter (Final Report). EPA/600/R-08/139F. Washington, DC:U.S. EPA.

762 U.S. EPA. 2018. Our Nation's Air. <https://gispub.epa.gov/air/trendsreport/2018/>

763 Val Martin, M., Heald, C. L., Lamarque, J.-F., Tilmes, S., Emmons, L. K. and Schichtel, B.
764 A.: How emissions, climate, and land use change will impact mid-century air quality over the
765 United States: a focus on effects at national parks, *Atmos. Chem. Phys.*, 15(5), 2805–2823,
766 doi:10.5194/acp-15-2805-2015, 2015.

767 Van der Werf, G. R., Randerson, J. T., Giglio, L., Collatz, G. J., Kasibhatla, P. S., and
768 Arellano, A. F.: Interannual variability in global biomass burning emissions from 1997 to
769 2004, *Atmos. Chem. Phys.*, 6, 3423-3441, DOI 737 10.5194/acp-6-3423-2006, 2006

770 Van Der Werf, G. R., Randerson, J. T., Giglio, L., Collatz, G. J., Mu, M., Kasibhatla, P. S.,
771 Morton, D. C., Defries, R. S., Jin, Y. and Van Leeuwen, T. T.: Global fire emissions and the
772 contribution of deforestation, savanna, forest, agricultural, and peat fires (1997-2009), *Atmos.*
773 *Chem. Phys.*, 10(23), 11707–11735, doi:10.5194/acp-10-11707-2010, 2010.

774 Van Donkelaar, A., R. V. Martin, M. Brauer, N. C. Hsu, R. A. Kahn, R. C. Levy, A.
775 Lyapustin, A. M. Sayer, and D. M. Winker. 2018. Global Annual PM_{2.5} Grids from MODIS,
776 MISR and SeaWiFS Aerosol Optical Depth (AOD) with GWR, 1998-2016. Palisades NY:

777 NASA Socioeconomic Data and Applications Center (SEDAC).
778 <https://doi.org/10.7927/H4ZK5DQS>. Accessed 16 November 2019.

779 Ward, D. S., Kloster, S., Mahowald, N. M., Rogers, B. M., Randerson, J. T. and Hess, P. G.:
780 The changing radiative forcing of fires: global model estimates for past, present and future,
781 *Atmos. Chem. Phys.*, 12(22), 10857–10886, doi:10.5194/acp-12-10857-2012, 2012.

782 Wotton, B. M., Flannigan, M. D., and Marshall, G. A.: Potential climate change impacts on
783 fire intensity and key wildfire suppression thresholds in Canada, *Environ. Res. Lett.*, 12,
784 095003, <https://doi.org/10.1088/1748-9326/aa7e6e>, 2017.

785 Westerling, A. L., Hidalgo, H. G., Cayan, D. R. and Swetnam, T. W.: Warming and Earlier
786 Spring Increase Western U.S. Forest Wildfire Activity, *Science* (80-.), 313(5789), 940 LP –
787 943, doi:10.1126/science.1128834, 2006.

788 Wotawa, G. and Trainer, M.: The Influence of Canadian Forest Fires on Pollutant
789 Concentrations in the United States, *Science* (80-.), 288(5464), 324 LP – 328,
790 doi:10.1126/science.288.5464.324, 2000.

791 Wu, Y., Arapi, A., Huang, J., Gross, B. and Moshary, F.: Intra-continental wildfire smoke
792 transport and impact on local air quality observed by ground-based and satellite remote
793 sensing in New York City, *Atmos. Environ.*, 187, 266–281,
794 doi:<https://doi.org/10.1016/j.atmosenv.2018.06.006>, 2018.

795 Xue, Z., Gupta, P., and Christopher, S.: Satellite-based estimation of the impacts of
796 summertime wildfires on PM_{2.5} concentration in the United States, *Atmos. Chem. Phys.*, 21,
797 11243–11256, <https://doi.org/10.5194/acp-21-11243-2021>, 2021.

798 Yang, P.-L., Y. Zhang, K. Wang, P. Doraiswamy, and S.-H. Cho, 2019, Health Impacts and
799 Cost-Benefit Analyses of Surface O₃ and PM_{2.5} over the U.S. under Future Climate and
800 Emission Scenarios, *Environmental Research*, 178, November 2019, 108687,
801 <https://doi.org/10.1016/j.envres.2019.108687>.

802 Yue, X., Mickley, L. J., Logan, J. A. and Kaplan, J. O.: Ensemble projections of wildfire
803 activity and carbonaceous aerosol concentrations over the western United States in the mid-
804 21st century, *Atmos. Environ.*, 77, 767–780,
805 doi:<https://doi.org/10.1016/j.atmosenv.2013.06.003>, 2013.

806 Zou, Y., Wang, Y., Ke, Z., Tian, H., Yang, J. and Liu, Y.: Development of a REgion-Specific
807 Ecosystem Feedback Fire (RESFire) Model in the Community Earth System Model, *J. Adv.
808 Model. Earth Syst.*, 11(2), 417–445, doi:10.1029/2018MS001368, 2019.

809 Zou, Y., Wang, Y., Qian, Y., Tian, H., Yang, J. and Alvarado, E.: Using CESM-RESFire to
810 understand climate–fire–ecosystem interactions and the implications for decadal climate
811 variability, *Atmos. Chem. Phys.*, 20, 995–1020, <https://doi.org/10.5194/acp-20-995-2020>,
812 2020.

813 Zhang, Y., P.-L. Yang, Y. Gao, R. L. Leung, and M. Bell, 2020, Health and Economic
814 Impacts of Air Pollution Induced by Climate Extremes over the Continental U.S.,
815 *Environmental International*, 143, 105921, <https://doi.org/10.1016/j.envint.2020.105921>.

816

817